Vision Research 51 (2011) 2176–2185

Contents lists available at SciVerse ScienceDirect

Vision Research

journal homepage: www.elsevier.com/locate/visres

Degeneration of cortical function in the Royal College of Surgeons rat

Carlos Gias *, Anthony Vugler, Jean Lawrence, Amanda Jayne Carr, Li Li Chen, Ahmed Ahmado, Ma'ayan Semo, Peter J. Coffey

Institute of Ophthalmology, University College London, 11-43 Bath Street, EC1V 9EL London, UK

ARTICLE INFO

Article history:
Received 24 May 2010
Received in revised form 13 June 2011
Available online 18 August 2011

Keywords:
Spatial frequency
Gratings
Optical imaging
Electrophysiology
Cortex

ABSTRACT

The purpose of the current study was to determine the progress of cortical functional degeneration in the Royal College of Surgeons (RCS) rat. Cortical responses were measured with optical imaging of intrinsic signals using gratings of various spatial frequencies. Subsequently, electrophysiological recordings were also taken across cortical layers in response to a pulse of broad-spectrum light. We found significant degeneration in the cortical processing of visual information as early as 4 weeks of age. These results show that degeneration in the cortical response of the RCS rat starts before development has been properly completed.

© 2011 Elsevier Ltd. All rights reserved.

1. Introduction

Age related macular degeneration and retinitis pigmentosa are human retinal diseases that result from defective retinal pigment epithelium (RPE) or photoreceptor cells, with a progressive loss of photoreceptors leading to severe visual impairment. The Royal College of Surgeons (RCS) rat also suffers from a defect in the retinal pigment epithelium cells which affects their ability to phagocytose rod outer segments (D'Cruz et al., 2000; Dowling & Sidman, 1962) and results in the gradual death of photoreceptors (LaVail & Battelle, 1975). Therefore, the RCS rat has been considered a suitable animal model to understand the progress of degeneration in retinal diseases and to develop therapies aimed at preserving visual function (Coffey et al., 2002; Lund et al., 2001; Tomita et al., 2007; Vugler et al., 2007). Previous studies have reported anatomical and neurochemical abnormalities by 2 weeks of age in the RCS rat (Davidorf et al., 1991; LaVail & Battelle, 1975). At this age, some aspects of retinal function already show signs of degeneration as measured with electroretinograms (ERG) (Dowling & Sidman, 1962; Fulton, 1983; Pinilla, Lund, & Sauve, 2004). Both ERG function (Bush, Hawks, & Sieving, 1995) and visual sensitivity at the superior colliculus (Girman, Wang, & Lund, 2005; Sauve et al., 2001; Sauve, Lu, & Lund, 2004) progressively degenerate over several months.

Primary visual cortex is a major visual centre in the brain for the processing of pattern visual information and preservation of cortical responses in this area is necessary for conscious vision. In order to understand how retinal degeneration impacts conscious perception, visual function needs to be assessed at the cortical level. Comparatively, few studies have specifically addressed cortical function in the RCS rat and only at an already advanced stage of degeneration (Gias et al., 2007; Girman, Wang, & Lund, 2003). Given the extensive use of this animal model in pre-clinical studies, it is important to establish the impact of retinal degeneration on the processing of visual stimuli in brain areas relevant to conscious perception. To our knowledge, there has not been a detailed investigation into the progression of cortical functional degeneration in a rodent model of retinal degeneration within the first postnatal months.

Multiunit activity recordings (MUA) give a measure of the output from a neuronal population (Legatt, Arezzo, & Vaughan, 1980) while local field potentials (LFP) are thought to be indicative of input and intracortical processing by a local neural population (Logothetis et al., 2001). There is also a close link between the electrical activity of a population of neurons and the local metabolic activity measured with optical imaging of intrinsic signals (Grinvald et al., 1986). This technique can indirectly measure simultaneously the neuronal activity of a relatively large area of the cortex and has been useful in determining the retinotopic

Abbreviations: c/d, cycles per degree of visual field; c/s, cycles per second; spk/s, spikes per second; COA, centre of activity; ERG, electroretinogram; LFP, local field potentials; MUA, multi-unit activity; RCS, Royal College of Surgeons; RPE, retinal pigment epithelium; SD, standard deviation.

* Corresponding author.

E-mail addresses: c.gias@ucl.ac.uk (C. Gias), a.vugler@ucl.ac.uk (A. Vugler), jean.lawrence@ucl.ac.uk (J. Lawrence), a.carr@ucl.ac.uk (A.J. Carr), smgxllc@ucl.ac.uk (L.L. Chen), ahmado73@yahoo.co.uk (A. Ahmado), m.semo@ucl.ac.uk (M. Semo), p.coffey@ucl.ac.uk (P.J. Coffey).

0042-6989/$ - see front matter © 2011 Elsevier Ltd. All rights reserved.
doi:10.1016/j.visres.2011.08.012

map in the rodent visual cortex (Gias et al., 2005; Kalatsky & Stryker, 2003; Schuett, Bonhoeffer, & Hubener, 2002) as well as the cortical response to pattern stimulation in several species (Heimel et al., 2007; Lu & Roe, 2007; Zhan, Ledgeway, & Baker, 2005) including the rat (Gias et al., 2007).

The main aim of the current study was to determine the extent of pattern-vision degeneration in the cortex as a result of retinal dystrophy in the RCS rat model. The tools used to address this line of investigation are electrophysiology and intrinsic optical imaging.

2. Methods

2.1. Animals

All animal care was in accordance with institutional and Home Office (UK) regulations and the UK Animals Scientific Procedures, Act 1986. Animals were kept in a 12-h dark/light cycle environment at a temperature of 22 °C with food and water ad libitum. Two groups of rats of either sex were used in this study at three different time points: dystrophic pigmented RCS (total $n = 22$: 9(P28–35), 6(P49–56), 7(P98–105)) and congenic control (total $n = 21$: 6(P28–35), 8(P49–56), 7(P98–105)). Optical imaging responses were measured in all the rats tested and additional electrophysiological recordings were also taken from a subset of the RCS (total $n = 18$: 8(P28–35), 5(P49–56), 5(P98–105)) and congenic control (total $n = 16$: 5(P28–35), 4(P49–56), 7(P98–105)) groups of rats.

2.2. Surgery

Subjects were anaesthetised with urethane (1.25 g/kg ip) and placed in a stereotaxic holder. A midline incision was made to expose the surface of the skull. The skull overlying right V1 was thinned to translucency with a dental drill under constant cooling with saline. A tracheotomy was performed to enable artificial ventilation (20% O_2, 80% N_2; 1–1.3 Hz). Blood oxygen saturation and heart rate were monitored non-invasively with a MouseOx (Starr Life Sciences Corp, Oakmont, PA, USA). Data presented in this study was taken with average blood oxygen saturation above 90%. Rectal temperature was monitored and maintained constant at 37.5 °C with a homeothermic blanket (Harvard Apparatus) throughout the duration of the experiment.

2.3. Visual stimulation

Following surgery, the rat was held steady using a mouth bar and tilted 20° in the inferior direction and the right eye covered to prevent stimulation. A calibrated (Minolta Chroma meter CS100) Dell Ultrasharp monitor 1905 FP of 75 Hz frame rate monitor was placed laterally 25 cm from the rat's left eye at 45° azimuth and 20° elevation to present visual stimuli generated using MATLAB software with Psychophysics Toolbox (Brainard, 1997; Pelli, 1997). Stimuli subtended 60 × 60° of visual field and consisted of either a flash of light flickering at 2 Hz or horizontal sinusoidal gratings of spatial frequencies between 0.05–0.7 c/d moving back and forth at 2 c/s presented during 2 s. The flickering flash of light of 64 cd/m^2 peak luminance was presented against a dim blank screen during periods of no stimulation (0.15 cd/m^2). The gratings had a 99% Michaelson contrast and were presented in a pseudo-random sequence against a background of matched luminance (32 cd/m^2) during periods of no stimulation. The eye was regularly monitored throughout to ensure the pupil was not dilated and for any signs of opacities. Subsequently, the rat's pupil was dilated using Tropicamide (1.0%) and electrophysiological recordings were then taken under a bright pulse of broad-spectrum white light of 2 log cds/m^2 delivered using a Lambda DG-4 (Linton Instrumentation, UK) projected onto a diffuser to visually stimulate the left eye for 10 ms over an area spanning ~130° of visual field. During the recovery periods the luminance was 0.01 cd/m^2. Each type of visual stimulus was presented 25 times during optical imaging and electrophysiological measurements. Eye drops (hypromellose, 0.3%) were regularly delivered to the rat's eye throughout the duration of the experiment to keep it moist.

2.4. Data collection

2.4.1. Single wavelength optical imaging

In order to perform single wavelength optical imaging the cortex was illuminated using a stabilised light source (Xenon arc lamp), using a narrow bandpass (10 nm Full Width-Half Maximum) interference filter with peak transmittance at 570 nm wavelength (Edmund Optics, York, UK). Frames were taken of cortex through the thinned skull at 15 Hz using a 12 bit, Dalsa 1M60 CCD camera (Dalsa, Waterloo, Canada) focused 700 μm below the cortical surface. Each frame was made of 128 × 128 pixels covering an area of ~5.8 × 5.8 mm. The period between stimuli was 18 s to allow the optical signal to return to baseline and frames were collected and stored over 13 s starting 8 s before stimulus onset. The data were averaged over 25 repetitions on a frame by frame basis before being subjected to further analysis.

2.4.2. Electrophysiological recordings

Once the optical imaging recordings were finished and the response location identified, a burr hole was drilled in the thinned skull at the centre of activity and a 16 channel electrode probe (100 μm spacing, Neuronexus Technologies, Miami, USA) inserted 1500 μm perpendicular to the surface. Electrical recordings were preamplified, collected and digitised at 6 kHz/16-bit precision, using a data acquisition device (RX5 Pentusa system, Tucker-Davis Technologies, Alachua, FL, USA). Data was continuously collected during the stimulation protocol and averaged over the 25 repetitions before further analysis was carried out.

2.5. Data analysis

2.5.1. Single wavelength optical imaging

The mean from each pixel was removed by its pre-stimulus average and further analysed by using a general linear model in a similar way as previously described (Gias et al., 2007; Mayhew et al., 1998).

The general linear model can be expressed as:

$$X = A\beta + e$$

where X represents the data matrix, A is the design matrix with a column for every factor represented in the model, β is the parameter matrix that represents the contribution that every effect has on the time series of each pixel and e is the error.

To explain the pixel's time-series changes, the response was modelled as a gamma distribution peaking at 3 s after stimulus onset. In order to model the spontaneous low frequency changes in the time-series (Mayhew et al., 1996) we used a sine and cosine signals of 0.08, 0.1 and 0.12 Hz and to account for possible deviations of the response's peak time the derivative of the modelled response was also used in the design matrix (Calhoun et al., 2004).

By applying regression analysis on the data we can obtain estimates of the response and a statistical indication of its variability (Gias et al., 2007). The ratio between the parameter estimate of the response and its standard deviation (the square root of its variance) was calculated as a measure of significant activation in terms of z scores. The centre of activity (COA) was calculated from those pixels exceeding a threshold of five standard deviations (SD)

and confirmed to be within V1 according to the stereotaxic brain atlas using bregmatic and sagittal sutures as visual landmarks (Paxinos & Watson, 1998) and fluoro-gold immunostaining (Supplementary Fig. 1). Given that the location of cortical activity was relatively unaffected by the spatial frequency (Supplementary Fig. 2), a fixed region of interest (ROI) centred at the COA was chosen for each animal to calculate the averaged optical imaging response across spatial frequencies. A circular ROI of 2 mm^2 spanning approximately 60% of the retinotopic projection of the visual stimulus (~30 μm/deg, Gias et al., 2005) was considered appropriate for measuring the average cortical response (Fig. 1). Given that low spatial frequencies have been shown to be more effective in eliciting behavioural and electrophysiological responses in non-dystrophic (Dean, 1978, 1981; Harnois, Bodis-Wollner, & Onofrj, 1984; Silveira, Heywood, & Cowey, 1987) and dystrophic RCS (Coffey et al., 2002; Gias et al., 2007) rats than high spatial frequencies, the ROI was calculated using the 0.05 c/d stimulus. If a cortical response was absent at this stimulus but still responsive to a flickering flash response, the latter was used to estimate the ROI. If no visual stimulus evoked an optical imaging response, a point within primary visual cortex at approximately −6.5 mm from bregma and 3.5 mm lateral from the sagittal suture was chosen instead as the COA.

2.5.2. Electrophysiology

The recorded signal was analysed offline using custom-made MATLAB software. The signal was divided into local field potential (LFP, μV) and multiunit activity (MUA, spikes per second: spk/s) by zero phase shift band-pass filtering in the 1–150 Hz range and the 300–3000 Hz range respectively. The firing rate of MUA data was calculated in 5 ms bins by spike counting at 3 SD above the baseline activity level (Jones et al., 2004). To quantify the response across layers, one representative electrode contact with the largest response was selected in each cortical layer. LFP (/MUA) onset latency for each layer was defined as the earliest significant (>3 SD) decrease (/increase) from baseline (−2 s to 0 s) that was maintained for at least 10 ms. The peak following stimulation was taken as the amplitude of the response.

2.6. Immunohistochemistry

2.6.1. Retina

Following the completion of imaging experiments, rats were perfused with 0.1 M phosphate buffered saline (PBS), followed by 4% paraformaldehyde (in PBS). Prior to rapid freezing in OCT imbedding compound, eyes were removed and cryoprotected by overnight incubation (at 4 °C) in 30% sucrose solution. Retinal tissue sections (20 μm) were cut on a cryostat and collected onto charged slides (BDH). For immunohistochemistry, all incubations were carried out in PBS containing 0.3% Triton X-100. Sections were blocked with 5% normal donkey serum for 2 h before overnight incubation with a combination of the following primary antibodies: rabbit anti-red/green (M/L) opsin (1:5000, Chemicon); mouse anti-rhodopsin (1D4, Abcam, Cambridge, UK); goat anti-blue (S) opsin (1:500, Santacruz Biotechnology, Heidelberg, Germany). Following an extensive wash in PBS, sections were then incubated in appropriate combinations of secondary antibodies. The secondary antibodies used were TRITC conjugated anti-rabbit, FITC anti-mouse and FITC anti-goat IgG (all cross-adsorbed to multiple species and purchased from Jackson ImmunoResearch). Following a final wash in PBS, sections were cover-slipped with Vectashield (Vector labs, Peterborough, UK).

As controls for secondary antibody specificity, some tissue was processed in parallel for immunofluorescence staining, with the omission of one or both primary antibodies. In these cases no signal was detectable. Additionally, immunostaining could be abolished following preadsorption of primary antibodies with the requisite blocking peptides. Fluorescent labelling was examined using a Zeiss 510 confocal microscope and LSM Image Browser software, retina structure was visualised concurrently using Normarski optics.

2.6.2. Brain

2.6.2.1. Fluoro-gold with SMI-32 co-labelling. A burr hole was drilled in the thinned skull at the COA as identified with optical imaging. The needle of a 10 μl Hamilton was inserted 700 μm perpendicular to the surface. 1 ml of a 3% solution of Fluoro-gold (FG; Fluorochrome Inc., Engelwood, CO) in 0.9% saline and 10% dimethylsulphoside was then injected. Subsequently, animals were perfused intracardially with a PBS flush followed by 4% paraformaldehyde in 0.1 M phosphate buffer. Brains were removed and cryoprotected overnight at 4 °C in a 30% sucrose solution (in 0.1 M PBS), and then frozen with a dry ice/acetone slurry. Coronal brain sections (30 μm thick) were cut on the cryostat and processed free-floating. Tissues were blocked for 2 h with 5% normal donkey serum (NDS) in PBS containing 0.3% Triton X-100 (PBS-TX) and subsequently incubated overnight in PBS-TX containing 1% NDS and mouse monoclonal primary anti-neurofilament heavy chain (SMI-32, Covance, 1:5000) followed by the secondary antibody (TRITC anti-mouse IgG, from Jackson ImmunoReseach). The neurofilament-H antibody was used to aid the identification of cytoarchitectural boundaries in the cortex (Van der Gucht, Hof, Van Brussel, Burnat, & Arckens, 2007). Sections were imaged on a Zeiss LSM 710 confocal microscope with a digital stage, tile images were stitched together and projected using Zeiss ZEN 2009 software.

2.6.3. Statistical methods

Analysis of variance (ANOVA) was used to compare the amplitude responses and onset latencies between control and RCS rats using SPSS 12 software. To identify the cortical layers that contribute most to the difference in activity between both groups at a particular age, post hoc *t*-tests were carried out using Bonferroni correction. Significance level was set at 0.05.

3. Results

3.1. Optical imaging response in the control and RCS rat

Brain activity following stimulation results in an increase in the cerebral blood volume leading to a reduction in the light reflected from the cortex, intrinsic signal. Animals were stimulated using a flickering flash of light at 2 Hz and gratings of spatial frequencies ranging from 0.05 to 0.7 c/d and brain activity was recorded from primary visual cortex. A pseudo-colour *z* scores map of cortical activation is shown in Fig. 1.

The visual stimulus causes a decrease of the intrinsic signal (increased blood volume) on the cortically active area during the initial 2–3 s after stimulus onset before peaking and subsequently returning to baseline. A large intrinsic signal response was reliably elicited in every control rat from every age group tested both using the flickering flash of light and moving gratings of low spatial frequencies. At higher spatial frequencies the cortical response was reduced in line with previous intrinsic imaging studies in other species (Gias et al., 2007; Heimel et al., 2007; Lu & Roe, 2007). Responses spanned a large area of the imaged window corresponding to rat V1 with decreasing amplitude in cortical regions closer to midline. In contrast, cortical responses in the RCS dystrophic group were in general less reliable and of lower amplitude. Up until P56, a cortical response was evoked in every RCS rat to the flickering flash whereas at P98–105 we did not observe clear changes in the intrinsic signal following stimulation in all the dystrophic rats.

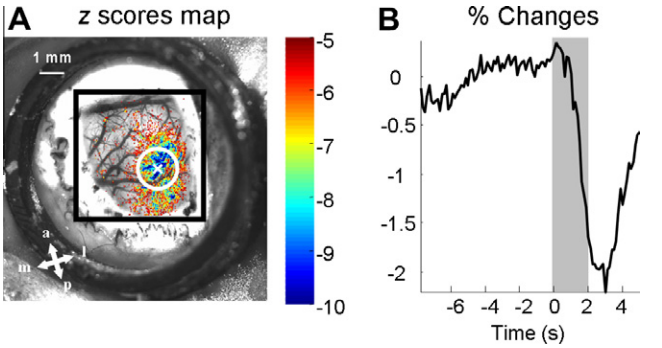

Fig. 1. Spatio-temporal response in a control rat to a grating stimulus of 0.05 c/d. (A) Pseudo-colour *z* scores response map superimposed to an anatomical picture of visual cortex taken at 570 nm. The white cross represents the COA and the white circle represents the 2 mm^2 area around the COA where the time series is averaged across pixels. a, anterior; p, posterior; m, medial; l, lateral. (B) Average time response following 2 s of visual stimulation. Grey shadow indicates the time when the stimulus was ON.

Examples of these responses are shown in Fig. 2. The pixels with the lowest *z* score values (largest in absolute value) in the *z* scores maps are represented as the darkest in the grey-scaled images and correspond to pixels with a maximal decrease in the intrinsic signal (maximal response) following stimulation. In order to quantify these observations, we computed the average time series of those pixels within a circular cortical region of 2 mm^2 centred at the COA (see methods). The time series for corresponding stimulus, age and group were then averaged across animals. The resulting averaged time series are plotted in Fig. 3A in response to a flickering flash stimulus. There is a decline of 37% in the average amplitude of the response between the youngest and oldest group of control animals with age although it does not reach significance (ANOVA, $F(2, 16) = 1.41$; $P = 0.344$). While the amplitude of the response was between 1.5–2.5% in the control animals, this was 1% or less in RCS dystrophic rats, being smallest at P98–105 (~0.5%). We found an overall statistical difference in the amplitude of the response between the RCS and control groups of rats (two-way ANOVA; factor 1: age, factor 2: group of rat; $F(1, 37) = 20.98$; $P < 0.001$). Post hoc *t*-test analysis showed a statistical difference at P98–105 using Bonferroni corrected *P* values ($P_{corr} < 0.05$). While the amplitude difference at P28–35 and P49–56 did not reach threshold, there was a trend towards it ($P_{corr} = 0.084$ and $P_{corr} = 0.141$ respectively).

In relation to the response to pattern stimulation, a comparison between both the RCS and the control group of rats showed an overall difference in the cortical responsiveness in the RCS rat to gratings stimulation (three-way ANOVA; factor 1: age, factor 2: group of rat, factor 3: spatial frequency; $F(1, 37) = 62.87$; $P < 0.001$). The responses across the spatial frequencies were greatly reduced not only in the older RCS rats but also in the young ones. Fig. 3B represents a comparison of the averaged time series across the different spatial frequencies. In the control group the amplitude of the response was ~1% or more following gratings stimulation at low and medium spatial frequencies. The response at high spatial frequencies was small in all the age groups although it got more prominent in older animals. By plotting the amplitude of the responses as a function of the spatial frequency in log units, they appear to be inversely but approximately linearly related

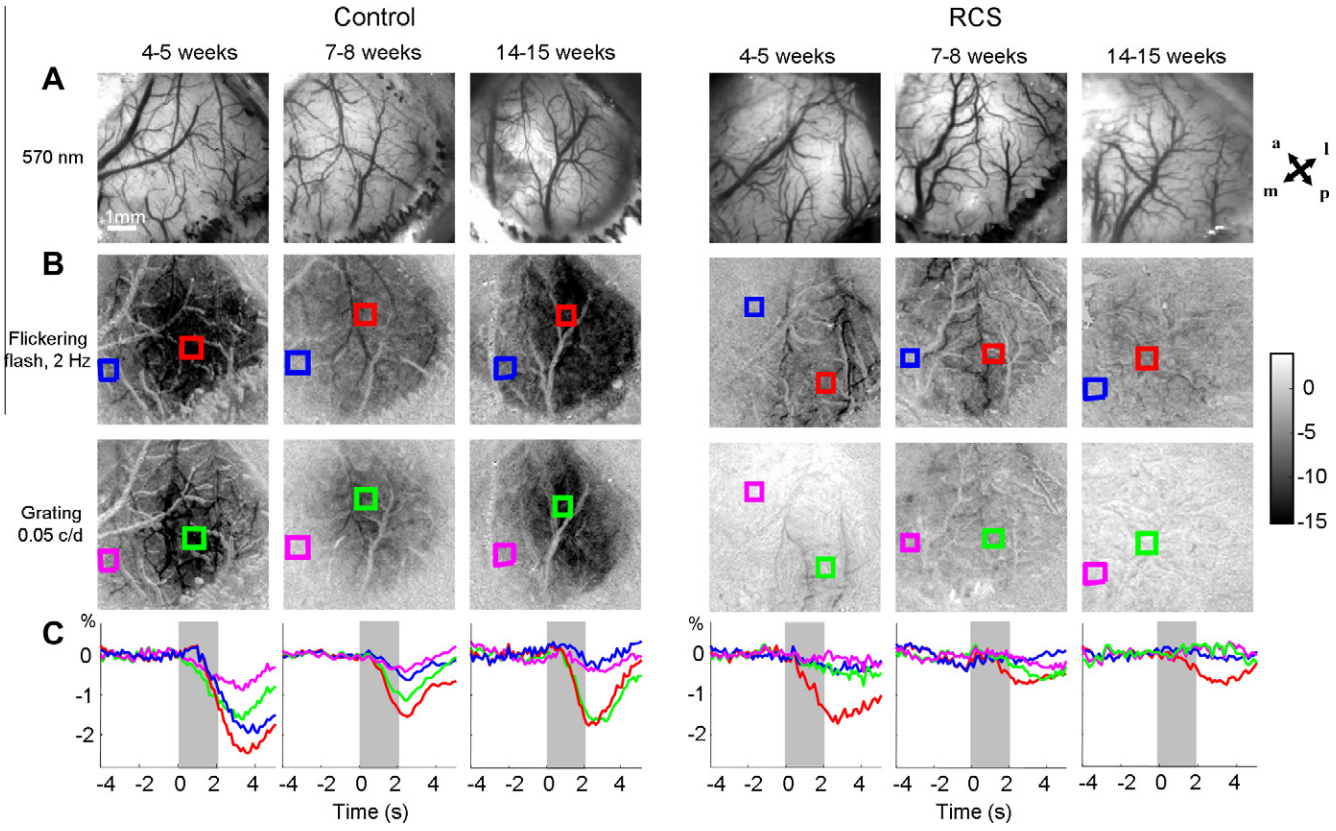

Fig. 2. Spatio-temporal responses of individual control and RCS dystrophic animals from different age groups following visual stimulation. (A) Thinned window overlying visual cortex as viewed using 570 nm light at the different age groups. a, anterior; p, posterior; m, medial; l, lateral. (B) *Z* scores maps following a flickering flash (2 Hz) and grating stimulation (0.05 c/d, 2 c/s). (C) Average time series across pixels from different regions of interest as shown in (B). Grey shadow indicates the time when the stimulus was ON. Scale bar in (A) applies to all images.

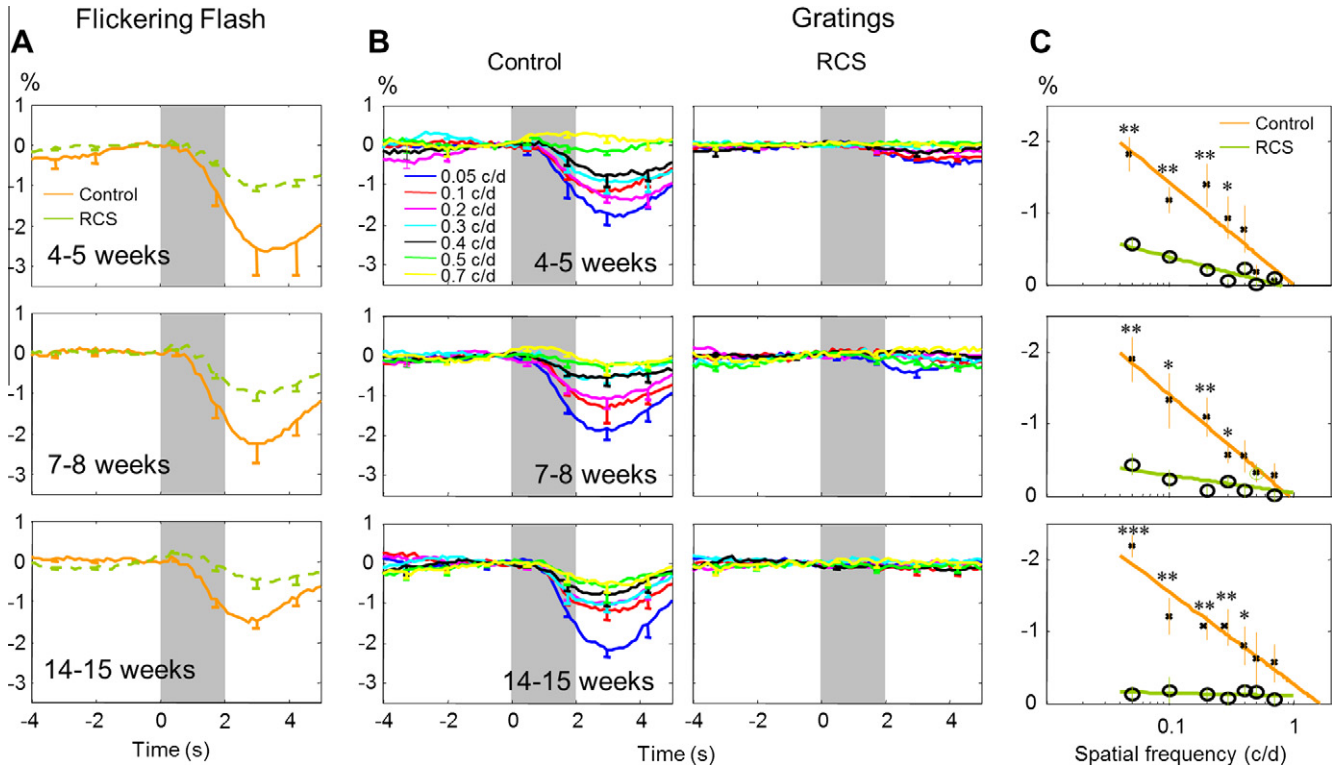

Fig. 3. Amplitude of the intrinsic signal response comparison between RCS dystrophic and control rats following stimulation. Error bars represent SEM. Grey shadow indicates the time when the stimulus was ON. (A) Time series responses averaged across animals to a flickering flash stimulus. (B) Time series responses averaged across animals to gratings at several spatial frequencies. (C) Amplitude of responses averaged across animals at several spatial frequencies (logarithmic representation). Asterisk gives an indication of the *P* value following independent samples *t*-test comparison between RCS and control groups of rats at the different spatial frequencies ($^{*}P < 0.05$; $^{**}P < 0.01$; $^{***}P < 0.001$).

(Fig. 3C). The amplitude of the responses data was fitted with a straight line using least squares. We calculated the R^2_{adj} value in order to give an indication of the goodness-of-fit and we found a reasonable good fit in the control animals across the different age groups ($R^2_{adj} > 0.8$, $P < 0.01$). This straight line was extrapolated to give an indication of the acuity of the animals using optical imaging. The line crosses the level of noise of the intrinsic signal (~0.2%) within the range of 0.67–1.14 c/d, in close similarity to previous rat studies (Dean, 1978, 1981; Harnois, Bodis-Wollner, & Onofrj, 1984; Silveira, Heywood, & Cowey, 1987). In the RCS dystrophic group we did not observe a response at high spatial frequencies at any age group. The amplitude of the response at low and medium spatial frequencies in the RCS group was less than 1% even in the P28–35 rats although a straight line fitted the data well at this age ($R^2_{adj} > 0.8$, $P < 0.01$) crossing the 0.2% level at 0.26 c/d. Responses to pattern stimulation were in most cases absent in the P49–56 and P98–105 RCS dystrophic groups and a straight line did not fit the data well ($R^2_{adj} < 0.3$, $P > 0.1$).

The response decrease pattern described here at increasing spatial frequencies does not depend on the COA location. Supplementary Fig. 3 shows that, despite lower responses, this phenomenon is also observed at cortical regions surrounding the COA. The size of the cortical area does not greatly affect the results either, with a twofold increase in the size of the ROI resulting in less than 10% change in the amplitude of the response (see Supplementary Fig. 4).

3.2. Electrophysiological response across cortical layers following a light pulse

We were interested in detecting any residual visual function at advanced cases of retinal degeneration. To achieve this, retina stimulation was maximised by dilating the pupil of the rat and delivering a bright pulse of broad spectrum light over a large area of the visual field. An initial increase in the LFP was recorded from the most superficial electrode channels (~<150 μm from surface) while negative initial deflections were seen in deeper recordings with the largest amplitudes found at ~500–800 μm below the cortical surface corresponding to lower layer III, layer IV and upper layer V (Fig 4) in agreement with previous rat studies (Heynen & Bear, 2001; Kenan-Vaknin & Teyler, 1994).

To quantify the response we compared the peak responses from supragranular (S), granular (G) and infragranular (I) layers between the dystrophic RCS and control rats at the different age groups. This type of stimulus was very reliable in evoking a cortical response even in the oldest RCS dystrophic rats tested and large responses were found up until P49–56 (Fig. 5). No statistical differences in the amplitudes of LFP (ANOVA, P28–35: $F(1, 11) = 1.53$, $P > 0.05$; P49–56: $F(1, 7) = 3.92$, $P > 0.05$) nor MUA (ANOVA, P28–35: $F(1, 11) = 1.04$, $P > 0.05$; P49–56: $F(1, 7) = 0.072$, $P > 0.05$) responses were found between control and RCS dystrophic rats younger than P49–56. At the age of P98–105, we found a significant reduction in the amplitude of the LFP response in the RCS rat in comparison to the control group (ANOVA, $F(1, 10) = 23.24$, $P < 0.01$). Equally, there was a significant reduction in the MUA response (ANOVA, $F(1, 10) = 17.51$, $P < 0.01$) at P98–105 with a reduction in the spiking rate of about one third the one measured at P49–56 across cortical layers. Both LFP and MUA responses were significantly reduced in the RCS rat at P98–105 across all the cortical layers (post hoc *t*-test, Bonferroni correction, $P < 0.05$).

3.3. Latency of the response

The speed of transmission of visual information from retina to visual cortex was assessed by measuring the latency of the

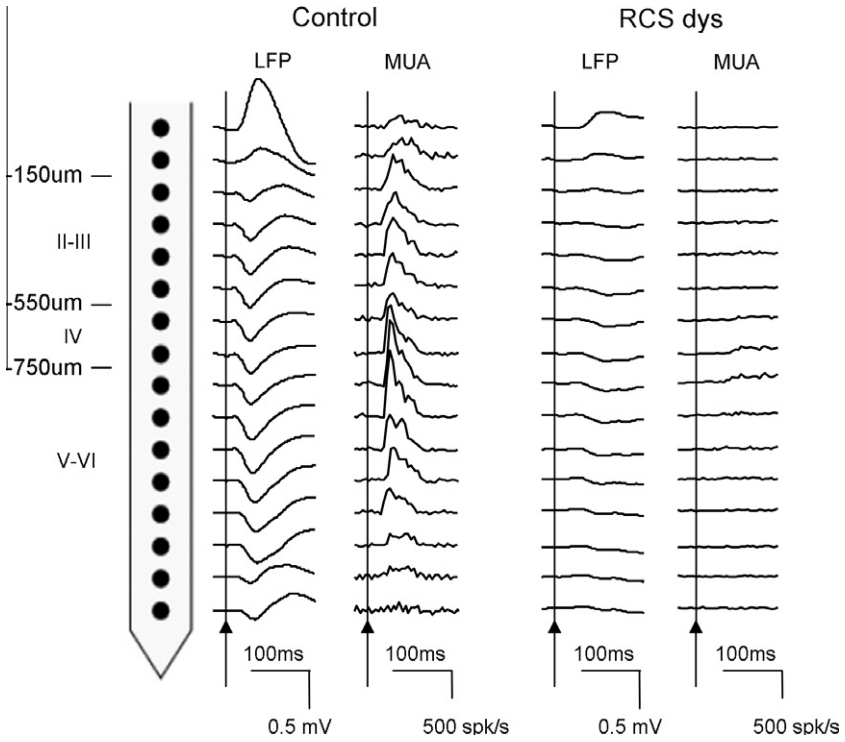

Fig. 4. LFP and MUA responses across cortical layers following a short pulse of bright white light (10 ms duration) in P98-105 control and P98–105 RCS dystrophic rats. Arrows indicate stimulus onset.

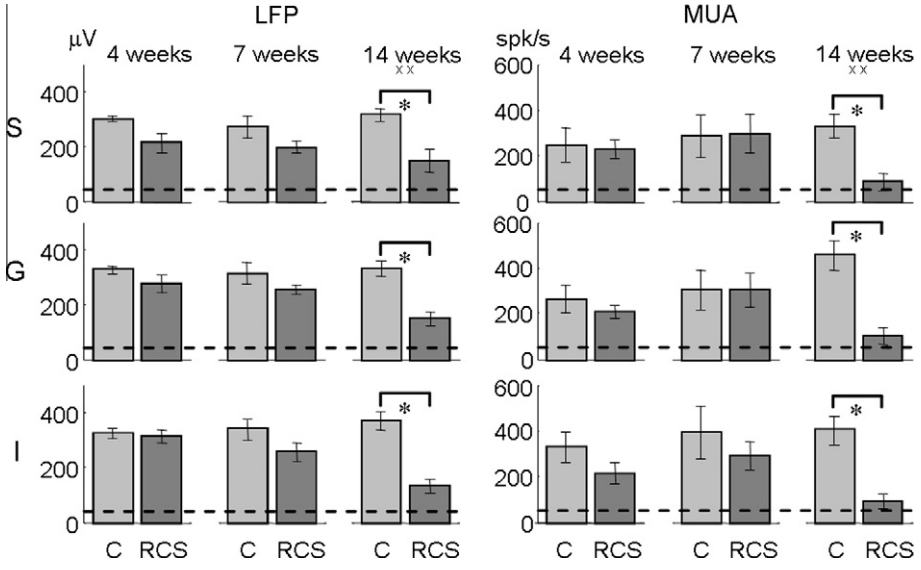

Fig. 5. LFP and MUA amplitude comparisons between RCS dystrophic and control rats following a short pulse of bright white light across the different age groups and cortical layers. S: supragranular layer, G: granular layer, I: infragranular layer. Error bars represent SEM. Discontinuous line represents the approximate level of background activity. The cross indicates a statistically significant difference at a particular age between both RCS and control groups of rats (repeated measures ANOVA, xx $P < 0.01$). Asterisk indicates a statistical difference between groups at a specific layer (post hoc t-test, Bonferroni correction, $^{*}P < 0.05$).

electrophysiological cortical response relative to the initiation of light stimulus. The onset latency of LFP and MUA in the control animals across cortical layers was within 25–35 ms remaining constant throughout the different age groups (Fig. 6). Instead, the onset latency in the P28–35 RCS rat was in the range of 35–50 ms. This difference was statistically significant (LFP: ANOVA, $F(1, 11) = 9.35$, $P < 0.05$; MUA: ANOVA, $F(1, 11) = 5.94$, $P < 0.05$) confirming that an increase in response latency occurs as early as P28–35 in the RCS rat. This effect is not limited to a cortical layer and statistical differences were seen across supragranular, granular and infragranular layers (post hoc t-test, Bonferroni correction, $P < 0.05$). The latency of the response progressively increased in the RCS rats with age and we found a delay of at least 60 ms from stimulus onset before the cortical response was evoked in the P98–105 dystrophic rats. This increase in the latency of the response was homogenous and statistically significant across the different cortical layers.

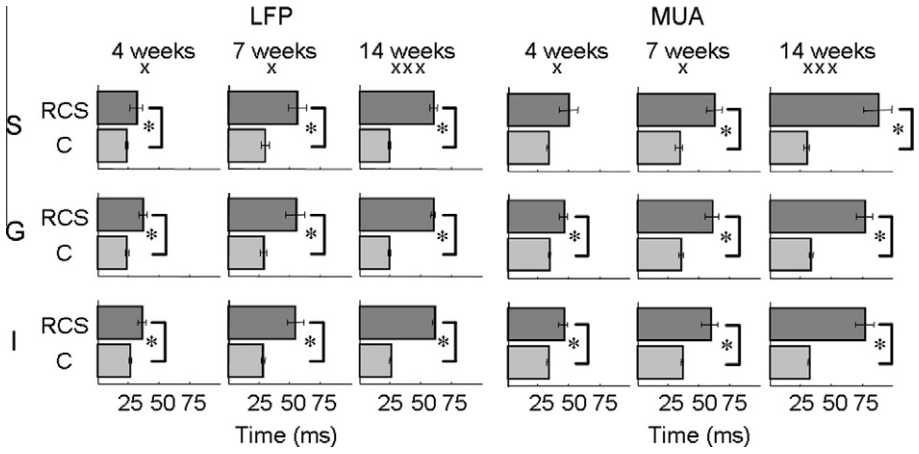

Fig. 6. Response latency comparisons of the peak LFP and MUA responses between RCS dystrophic and control (C) rats following a short pulse of bright white light across the different age groups and cortical layers. S: supragranular layer, G: granular layer, I: infragranular layer. Error bars represent SEM. Cross indicates a statistically significant difference at a particular age between both RCS and control groups of rats (repeated measures ANOVA, x $P < 0.05$; xxx $P < 0.001$). Asterisk indicates a statistical difference between groups at a specific layer (post hoc *t*-test, Bonferroni correction, $P < 0.05$).

4. Discussion

4.1. Early degeneration in the cortical processing of visual patterns in the RCS rat

This study has shown a pronounced reduction in the cortical processing of pattern stimulation over a broad range of spatial frequencies in the RCS rat at all the age groups tested. As shown in Supplementary Fig. 5 and in agreement with more detailed anatomical and functional studies (Cuenca et al., 2005; Davidorf et al., 1991; Dowling & Sidman, 1962; Girman, Wang, & Lund, 2005; Machida et al., 2008), retinal degeneration affecting rod function has started by 4–5 weeks of age in the RCS rat with an increase in the debris zone followed by disorganisation of opsin expression with age. It is less clear the extent that the cone system has been affected at this young age. We have only seen clear degeneration in the distribution of cone opsin across layers from 7 to 8 weeks and previous studies have suggested that there is normal maturation of the cone system (Pinilla, Lund, & Sauve, 2004). However, other detailed studies have shown morphological changes in cone transducin labelled cells (Cuenca et al., 2005) and functional abnormalities in the cone system (Machida et al., 2008) by 4–5 weeks. In addition to photoreceptor degeneration, the neural retina in the RCS is also affected. By P31, the oscillatory potential component of the ERG is reduced by half its amplitude suggesting a rapid change in amacrine cell circuitry (Cuenca et al., 2005). However, the impact of these early changes on higher visual structures cannot be inferred from these results.

In this study we have also demonstrated that cortically mediated processing of image-forming visual information is already compromised by 4–5 weeks. According to previous studies in the rat, cortical processing to pattern stimulation does not develop fully until ~6 weeks postnatally (Fagiolini et al., 1994; Stafford, 1984) or even longer (Guire, Lickey, & Gordon, 1999). The comparatively larger intrinsic signal responses at the highest spatial frequencies reported here in control animals older than 4–5 weeks also supports the view that visual acuity has not fully developed by this age. Neuronal inhibition plays a major role in the cortical processing of gratings (De Valois & Tootell, 1983; Sillito, 1979; Worgotter & Koch, 1991) and its progressive development in the rat up to 6 weeks of age (Huang et al., 1999; Yamashita et al., 2003) could potentially amplify the visual responses to this type of stimulus. One possible mechanism that could explain this would be the development of inhibitory Off subregions in simple cortical neurons with a receptive field structure matching the spatial frequency of the visual stimulus through either intracortical inhibitory neurons (Hirsch'03) or feedback from higher order visual centres (Hupe et al., 1998). Neurotrophic factors appear to be important in the development of visual acuity (Huang et al., 1999). There are substantial neurotrophic factor abnormalities in the young RCS rat affecting the retina (Amendola, Fiore, & Aloe, 2003; Fletcher & Kalloniatis, 1997; Hankins & Ikeda, 1994; Kalloniatis & Tomisich, 1999), the geniculate nucleus and visual cortex (Amendola, Fiore, & Aloe, 2003) as early as 8 days postnatally. It is therefore plausible that an abnormal concentration of such factors in the neural structures of RCS rats could impede proper neural development. Because the RCS rat has been routinely employed for pre-clinical studies (Coffey et al., 2002; Lund et al., 2001), it is important to take into account the limitations of this rodent model for preserving normal visual function. Indeed, the effectiveness of a therapeutic intervention to preserve visual function is likely to be strongly influenced by the lack of normal development of rod/cone function. Therefore, we conclude that extrapolation of results from RCS studies to human patients with late-onset retinal degeneration may actually under-estimate the potential therapeutic benefit of the various cellular/molecular strategies tested to date (Coffey et al., 2002; Lund et al., 2001; Tomita et al., 2007).

4.2. Degeneration in the cortical processing of visual patterns in the adult RCS rat

In this study we have shown the reduced capability of the adult RCS rat to cortically process visual patterns with a complete loss. In contrast, a previous study in the old RCS rat (>P120) using single unit recordings has shown that, while infrequently, some cortical neurons have the capability to respond to gratings (Girman, Wang, & Lund, 2003). Methodological differences are likely to account for this disparity. Given that optical imaging mainly reflects input and intracortical processing by a neural population (Sheth et al., 2005), the output of a sparse population of neurons might not be effective enough to evoke a measurable optical imaging response.

Behavioural tests have been used in the past to study the degeneration of visual perception in the RCS rat with some reports showing that pattern discrimination can last up to 3 months (Hetherington et al., 2000) in line with our results, while others report that it extends up to 11 months of age (McGill et al., 2004). While visual stimulation differences can account for some

variability in the results across studies, behavioural tests can also be potentially more sensitive than optical imaging measurements. The response of a small population of cortical neurons might be below the detection threshold of optical imaging particularly in an anaesthetised preparation but sufficient to trigger an animal behaviour. In addition, the rat superior colliculus is the main recipient of retinofugal projections receiving input from virtually all ganglion cells. This input enables the superior colliculus to resolve gratings of up to 0.7 c/d (Dean, 1981) or even higher (Prevost, Lepore, & Guillemot, 2007) and has been involved in behavioural tests of pattern discrimination (Douglas et al., 2005). Therefore, it is also possible that residual function at the superior colliculus is preserved longer than at the visual cortex in the presence of retinal degeneration, eliciting a pattern-mediated behavioural response. To date, behavioural tests have been widely used to assess visual perception in rodent models of retinal disease and to test the efficacy of various treatments (Coffey et al., 2002; Ivanova & Pan, 2009; Lu et al., 2009; Tomita et al., 2007). However, given that the visual cortex is not the only visual structure that could mediate the measured behavioural responses, visual perception readouts using this approach does not necessarily translate to cortically-mediated conscious human perception. Therefore, we believe that studying the function of this brain area directly might provide data that is more applicable to human studies of visual perception.

4.3. Degeneration in the amplitude of the response to temporal changes in luminance level

Our results have shown evidence of a decline in the responsiveness to both flickering flash and short pulses of light by 4–5 weeks. As we and others (LaVail & Battelle, 1975) have shown, this loss of function corresponds closely with a reduced outer nuclear layer thickness from 4 to 8 weeks. This pathology results in the progressive degeneration in rod and cone function with a large reduction of the *b*-wave and loss of the *a*-wave by ~P50 (Bush, Hawks, & Sieving, 1995). It is worth noting that while at 4–5 weeks the cortical pattern response was severely compromised, the reduction of the response to temporal changes in luminance level was not pronounced until 7–8 weeks despite the loss of photoreceptor function. A number of different possibilities could explain this result. The certain decline in the cortical response to spatially uniform stimuli with age in the normal animal found in this study could reflect increased inhibitory-mediated centre surround antagonism. A visual input reduction might result in neurotrophic factor deficits and compromise the normal development of inhibitory connections that could lead to the preservation of the cortical response to spatially uniform stimulation while impairing the ability to respond to gratings at a normal level. Alternatively, an expansion of the cortical neuron receptive fields might prevent them from resolving the gratings while increasing the responsiveness to temporal changes in luminance level. Like the RCS rat, the P23H rat also has a genetic defect which results in the progressive loss of rod and cone function (Machida et al., 2000; Pinilla, Lund, & Sauve, 2005) and it has been suggested that changes in synaptic connectivity between the photoreceptors and bipolar cells in the retina might compensate for the loss of visual input. Given the similarities between these animal models, one would also expect a level of compensation in the RCS rat retina. While ganglion cell acuity was well preserved and no expansion of the corresponding receptive fields was found within the initial 3 months of life (Pu, Xu, & Zhang, 2006), the drastic reduction in the signal to noise ratio and/or the number of ON cells (Pu, Xu, & Zhang, 2006) could potentially disrupt the integration, transmission or processing of this signal at higher levels of the visual system. Lack of correlation between retinal and cortical acuity has been shown to occur due to abnormal visual development such as in amblyopia (Hess, 2001), because of BDNF deficits in the cortex post-development (Heimel et al., 2010) or during ageing (Spear, 1993). There is substantial evidence supporting the view that a visual input impairment results in an initial loss of functional activation in the corresponding cortical projection followed by an expansion of the activation to the deafferented cortical regions from neighbouring areas (Baker et al., 2005; Calford et al., 2005; Kaas, 2002). A similar phenomenon was also observed in the RCS rat visual cortex several months after retinal transplantation (Girman, Wang, & Lund, 2003). This could be due to underlying structural changes (Keck et al., 2008) and/or the reinforcement of the synaptic connections following loss of visual input of those neurons that are still active by either Hebbian or homeostatic synaptic plasticity mechanisms (Pozo & Goda, 2010).

Identifying the mechanism or mechanisms underlying the cortical changes after visual input deficits is a complex and controversial area of research (Wandell & Smirnakis, 2009). In addition to plastic changes, the enlargement of V1 responses could have a different origin such as intrinsic lateral connections or feedback from extrastriate regions. However, given the extensive and prolonged reduction of the visual input it is likely that some form of compensation would also take place in the RCS rat. Given that our results have shown strong spiking activity in input layer IV, a compensatory mechanism could originate, at least partially, in subcortical structures such as the lateral geniculate nucleus.

By ~P100, the majority of the photoreceptors have disappeared in the RCS rat (LaVail & Battelle, 1975), the *b*-wave is lost (Bush, Hawks, & Sieving, 1995; Machida et al., 2008) and there is widespread loss in the visual sensitivity of neurons at the superior colliculus (Sauve et al., 2001). At this age we also found a very substantial reduction in the amplitude of the optical imaging and electrophysiological (LFP and MUA) response using either the flickering flash or the pulse of light. This would suggest that the compensatory mechanism would no longer able to preserve cortical function to the level found in younger animals.

4.4. Degeneration in the response latency

Increases in response latency are relevant to the study of retinal disease, in particular, increased ERG latencies have been reported in patients suffering from retinitis pigmentosa (Hamasaki et al., 2002; Janaky et al., 2008; Sandberg, Sullivan, & Berson, 1981). This measure has also been shown to be a good indicator of functional preservation in the retina following therapeutic intervention (Sauve, Pinilla, & Lund, 2006). Our study has shown that the cortical response latency in control animals remained constant after P28–35, in agreement with previous ERG studies showing developmental changes stopping after P25 in the rat (Fulton, 1983). In comparison, the RCS rat displays response latency increases even at P25–28 in the retina (Deshpande et al., 1992; Fulton, 1983). Longer response latencies have also been detected in other visual structures in the RCS rat such as the superior colliculus (Sauve et al., 2002, 2001). Previous studies have not addressed the speed of transmission of visual information from the retina to the visual cortex. Here, we have shown that there is an increase in the cortical response latency in the RCS rat as early as P28–35 postnatally and it increases as the retinal degeneration progresses. The increase in latency suggests that the speed of neural transmission has been compromised in the cone system. Our findings showing an increase in the latency of the response present at the input layer IV, suggests that this phenomenon originates in pre-cortical structures.

5. Conclusion

The ability of a patient suffering from retinal disease to perceive the fine details of a visual scene depends on the capacity of the

visual cortex to process spatial patterns. The RCS rat has been extensively used in the past as an animal model to study retinal degeneration. This model has been assumed, by behavioural outputs, to develop normal visual function before degenerating as a result of the disease. However, no study has previously addressed the RCS rat's ability to process grating information in the cortex before the visual system is fully developed. The present study shows that this rat model fails to reach a normal cortical response level to pattern stimulation or luminance changes, with normal development compromised before maturity is attained.

Acknowledgment

This work was funded by the London Project to Cure Blindness.

Appendix A. Supplementary material

Supplementary data associated with this article can be found, in the online version, at doi:10.1016/j.visres.2011.08.012.

References

Amendola, T., Fiore, M., & Aloe, L. (2003). Postnatal changes in nerve growth factor and brain derived neurotrophic factor levels in the retina, visual cortex, and geniculate nucleus in rats with retinitis pigmentosa. *Neuroscience Letters, 345*(1), 37–40.

Baker, C. I., Peli, E., Knouf, N., & Kanwisher, N. G. (2005). Reorganization of visual processing in macular degeneration. *Journal of Neuroscience, 25*(3), 614–618.

Brainard, D. H. (1997). The psychophysics toolbox. *Spatial Vision, 10*(4), 433–436.

Bush, R. A., Hawks, K. W., & Sieving, P. A. (1995). Preservation of inner retinal responses in the aged Royal College of Surgeons rat. Evidence against glutamate excitotoxicity in photoreceptor degeneration. *Investigative Ophthalmology and Visual Science, 36*(10), 2054–2062.

Calford, M. B., Chino, Y. M., Das, A., Eysel, U. T., Gilbert, C. D., Heinen, S. J., et al. (2005). Neuroscience: Rewiring the adult brain. *Nature, 438*(7065), E3 (discussion E3-4).

Calhoun, V. D., Stevens, M. C., Pearlson, G. D., & Kiehl, K. A. (2004). FMRI analysis with the general linear model: Removal of latency-induced amplitude bias by incorporation of hemodynamic derivative terms. *Neuroimage, 22*(1), 252–257.

Coffey, P. J., Girman, S., Wang, S. M., Hetherington, L., Keegan, D. J., Adamson, P., et al. (2002). Long-term preservation of cortically dependent visual function in RCS rats by transplantation. *Nature Neuroscience, 5*(1), 53–56.

Cuenca, N., Pinilla, I., Sauve, Y., & Lund, R. (2005). Early changes in synaptic connectivity following progressive photoreceptor degeneration in RCS rats. *European Journal of Neuroscience, 22*(5), 1057–1072.

Davidorf, F. H., Mendlovic, D. B., Bowyer, D. W., Gresak, P. M., Foreman, B. C., Werling, K. T., et al. (1991). Pathogenesis of retinal dystrophy in the Royal College of Surgeons rat. *Annals of Ophthalmology, 23*(3), 87–94.

D'Cruz, P. M., Yasumura, D., Weir, J., Matthes, M. T., Abderrahim, H., LaVail, M. M., et al. (2000). Mutation of the receptor tyrosine kinase gene Mertk in the retinal dystrophic RCS rat. *Human Molecular Genetics, 9*(4), 645–651.

De Valois, K. K., & Tootell, R. B. (1983). Spatial-frequency-specific inhibition in cat striate cortex cells. *Journal of Physiology, 336*, 359–376.

Dean, P. (1978). Visual acuity in hooded rats: Effects of superior collicular or posterior neocortical lesions. *Brain Research, 156*(1), 17–31.

Dean, P. (1981). Grating detection and visual acuity after lesions of striate cortex in hooded rats. *Experimental Brain Research, 43*(2), 145–153.

Deshpande, S., Thompson, M., Parker, J. A., & Abrahamson, E. W. (1992). Study of retinal dystrophy in RCS rats: A comparison of Mg-ATP dependent light scattering activity and ERG b-wave. *Vision Research, 32*(3), 425–432.

Douglas, R. M., Alam, N. M., Silver, B. D., McGill, T. J., Tschetter, W. W., & Prusky, G. T. (2005). Independent visual threshold measurements in the two eyes of freely moving rats and mice using a virtual-reality optokinetic system. *Visual Neuroscience, 22*(5), 677–684.

Dowling, J. E., & Sidman, R. L. (1962). Inherited retinal dystrophy in the rat. *Journal of Cell Biology, 14*, 73–109.

Fagiolini, M., Pizzorusso, T., Berardi, N., Domenici, L., & Maffei, L. (1994). Functional postnatal development of the rat primary visual cortex and the role of visual experience: Dark rearing and monocular deprivation. *Vision Research, 34*(6), 709–720.

Fletcher, E. L., & Kalloniatis, M. (1997). Neurochemical development of the degenerating rat retina. *Journal of Comparative Neurology, 388*(1), 1–22.

Fulton, A. B. (1983). Background adaptation in RCS rats. *Investigative Ophthalmology and Visual Science, 24*(1), 72–76.

Gias, C., Hewson-Stoate, N., Jones, M., Johnston, D., Mayhew, J. E., & Coffey, P. J. (2005). Retinotopy within rat primary visual cortex using optical imaging. *Neuroimage, 24*(1), 200–206.

Gias, C., Jones, M., Keegan, D., Adamson, P., Greenwood, J., Lund, R., et al. (2007). Preservation of visual cortical function following retinal pigment epithelium transplantation in the RCS rat using optical imaging techniques. *European Journal of Neuroscience, 25*(7), 1940–1948.

Girman, S. V., Wang, S., & Lund, R. D. (2003). Cortical visual functions can be preserved by subretinal RPE cell grafting in RCS rats. *Vision Research, 43*(17), 1817–1827.

Girman, S. V., Wang, S., & Lund, R. D. (2005). Time course of deterioration of rod and cone function in RCS rat and the effects of subretinal cell grafting: A light- and dark-adaptation study. *Vision Research, 45*(3), 343–354.

Grinvald, A., Lieke, E., Frostig, R. D., Gilbert, C. D., & Wiesel, T. N. (1986). Functional architecture of cortex revealed by optical imaging of intrinsic signals. *Nature, 324*(6095), 361–364.

Guire, E. S., Lickey, M. E., & Gordon, B. (1999). Critical period for the monocular deprivation effect in rats: Assessment with sweep visually evoked potentials. *Journal of Neurophysiology, 81*(1), 121–128.

Hamasaki, D. I., Liu, M., Qiu, H., Fujiwara, E., & Lam, B. L. (2002). The *a*-wave latency in control subjects and patients with retinal diseases. *Japanese Journal of Ophthalmology, 46*(4), 433–442.

Hankins, M., & Ikeda, H. (1994). Early abnormalities of retinal dopamine pathways in rats with hereditary retinal dystrophy. *Documenta Ophthalmologica, 86*(3), 325–334.

Harnois, C., Bodis-Wollner, I., & Onofrj, M. (1984). The effect of contrast and spatial frequency on the visual evoked potential of the hooded rat. *Experimental Brain Research, 57*(1), 1–8.

Heimel, J. A., Hartman, R. J., Hermans, J. M., & Levelt, C. N. (2007). Screening mouse vision with intrinsic signal optical imaging. *European Journal of Neuroscience, 25*(3), 795–804.

Heimel, J. A., Saiepour, M. H., Chakravarthy, S., Hermans, J. M., & Levelt, C. N. (2010). Contrast gain control and cortical TrkB signaling shape visual acuity. *Nature Neuroscience, 13*(5), 642–648.

Hess, R. F. (2001). Amblyopia: Site unseen. *Clinical and Experimental Optometry, 84*(6), 321–336.

Hetherington, L., Benn, M., Coffey, P. J., & Lund, R. D. (2000). Sensory capacity of the Royal College of Surgeons rat. *Investigative Ophthalmology and Visual Science, 41*(12), 3979–3983.

Heynen, A. J., & Bear, M. F. (2001). Long-term potentiation of thalamocortical transmission in the adult visual cortex in vivo. *Journal of Neuroscience, 21*(24), 9801–9813.

Huang, Z. J., Kirkwood, A., Pizzorusso, T., Porciatti, V., Morales, B., Bear, M. F., et al. (1999). BDNF regulates the maturation of inhibition and the critical period of plasticity in mouse visual cortex. *Cell, 98*(6), 739–755.

Hupe, J. M., James, A. C., Payne, B. R., Lomber, S. G., Girard, P., & Bullier, J. (1998). Cortical feedback improves discrimination between figure and background by V1, V2 and V3 neurons. *Nature, 394*(6695), 784–787.

Ivanova, E., & Pan, Z. H. (2009). Evaluation of the adeno-associated virus mediated long-term expression of channelrhodopsin-2 in the mouse retina. *Molecular Vision, 15*, 1680–1689.

Janaky, M., Palffy, A., Horvath, G., Tuboly, G., & Benedek, G. (2008). Pattern-reversal electroretinograms and visual evoked potentials in retinitis pigmentosa. *Documenta Ophthalmologica, 117*(1), 27–36.

Jones, M., Hewson-Stoate, N., Martindale, J., Redgrave, P., & Mayhew, J. (2004). Nonlinear coupling of neural activity and CBF in rodent barrel cortex. *Neuroimage, 22*(2), 956–965.

Kaas, J. H. (2002). Sensory loss and cortical reorganization in mature primates. *Progress in Brain Research, 138*, 167–176.

Kalatsky, V. A., & Stryker, M. P. (2003). New paradigm for optical imaging: Temporally encoded maps of intrinsic signal. *Neuron, 38*(4), 529–545.

Kalloniatis, M., & Tomisich, G. (1999). Amino acid neurochemistry of the vertebrate retina. *Progress in Retinal and Eye Research, 18*(6), 811–866.

Keck, T., Mrsic-Flogel, T. D., Vaz Afonso, M., Eysel, U. T., Bonhoeffer, T., & Hubener, M. (2008). Massive restructuring of neuronal circuits during functional reorganization of adult visual cortex. *Nature Neuroscience, 11*(10), 1162–1167.

Kenan-Vaknin, G., & Teyler, T. J. (1994). Laminar pattern of synaptic activity in rat primary visual cortex: Comparison of in vivo and in vitro studies employing the current source density analysis. *Brain Research, 635*(1–2), 37–48.

LaVail, M. M., & Battelle, B. A. (1975). Influence of eye pigmentation and light deprivation on inherited retinal dystrophy in the rat. *Experimental Eye Research, 21*(2), 167–192.

Legatt, A. D., Arezzo, J., & Vaughan, H. G. Jr., (1980). Averaged multiple unit activity as an estimate of phasic changes in local neuronal activity: Effects of volume-conducted potentials. *Journal of Neuroscience Methods, 2*(2), 203–217.

Logothetis, N. K., Pauls, J., Augath, M., Trinath, T., & Oeltermann, A. (2001). Neurophysiological investigation of the basis of the fMRI signal. *Nature, 412*(6843), 150–157.

Lu, B., Malcuit, C., Wang, S., Girman, S., Francis, P., Lemieux, L., et al. (2009). Long-term safety and function of RPE from human embryonic stem cells in preclinical models of macular degeneration. *Stem Cells, 27*(9), 2126–2135.

Lu, H. D., & Roe, A. W. (2007). Optical imaging of contrast response in Macaque monkey V1 and V2. *Cerebral Cortex, 17*(11), 2675–2695.

Lund, R. D., Kwan, A. S., Keegan, D. J., Sauve, Y., Coffey, P. J., & Lawrence, J. M. (2001). Cell transplantation as a treatment for retinal disease. *Progress in Retinal and Eye Research, 20*(4), 415–449.

Machida, S., Kondo, M., Jamison, J. A., Khan, N. W., Kononen, L. T., Sugawara, T., et al. (2000). P23H rhodopsin transgenic rat: Correlation of retinal function with histopathology. *Investigative Ophthalmology and Visual Science, 41*(10), 3200–3209.

Machida, S., Raz-Prag, D., Fariss, R. N., Sieving, P. A., & Bush, R. A. (2008). Photopic ERG negative response from amacrine cell signaling in RCS rat retinal degeneration. *Investigative Ophthalmology and Visual Science, 49*(1), 442–452.

Mayhew, J. E., Askew, S., Zheng, Y., Porrill, J., Westby, G. W., Redgrave, P., et al. (1996). Cerebral vasomotion: A 0.1-Hz oscillation in reflected light imaging of neural activity. *Neuroimage, 4*(3 Pt 1), 183–193.

Mayhew, J., Hu, D., Zheng, Y., Askew, S., Hou, Y., Berwick, J., et al. (1998). An evaluation of linear model analysis techniques for processing images of microcirculation activity. *Neuroimage, 7*(1), 49–71.

McGill, T. J., Douglas, R. M., Lund, R. D., & Prusky, G. T. (2004). Quantification of spatial vision in the Royal College of Surgeons rat. *Investigative Ophthalmology and Visual Science, 45*(3), 932–936.

Paxinos, G., & Watson, C. (1998). *The rat brain in stereotaxic coordinates* (4th ed). San Diego: Academic Press.

Pelli, D. G. (1997). The VideoToolbox software for visual psychophysics: Transforming numbers into movies. *Spatial Vision, 10*(4), 437–442.

Pinilla, I., Lund, R. D., & Sauve, Y. (2004). Contribution of rod and cone pathways to the dark-adapted electroretinogram (ERG) b-wave following retinal degeneration in RCS rats. *Vision Research, 44*(21), 2467–2474.

Pinilla, I., Lund, R. D., & Sauve, Y. (2005). Enhanced cone dysfunction in rats homozygous for the P23H rhodopsin mutation. *Neuroscience Letters, 382*(1–2), 16–21.

Pozo, K., & Goda, Y. (2010). Unraveling mechanisms of homeostatic synaptic plasticity. *Neuron, 66*(3), 337–351.

Prevost, F., Lepore, F., & Guillemot, J. P. (2007). Spatio-temporal receptive field properties of cells in the rat superior colliculus. *Brain Research, 1142*, 80–91.

Pu, M., Xu, L., & Zhang, H. (2006). Visual response properties of retinal ganglion cells in the Royal College of Surgeons dystrophic rat. *Investigative Ophthalmology and Visual Science, 47*(8), 3579–3585.

Sandberg, M. A., Sullivan, P. L., & Berson, E. L. (1981). Temporal aspects of the dark-adapted cone *a*-wave in retinitis pigmentosa. *Investigative Ophthalmology and Visual Science, 21*(5), 765–769.

Sauve, Y., Girman, S. V., Wang, S., Keegan, D. J., & Lund, R. D. (2002). Preservation of visual responsiveness in the superior colliculus of RCS rats after retinal pigment epithelium cell transplantation. *Neuroscience, 114*(2), 389–401.

Sauve, Y., Girman, S. V., Wang, S., Lawrence, J. M., & Lund, R. D. (2001). Progressive visual sensitivity loss in the Royal College of Surgeons rat: Perimetric study in the superior colliculus. *Neuroscience, 103*(1), 51–63.

Sauve, Y., Lu, B., & Lund, R. D. (2004). The relationship between full field electroretinogram and perimetry-like visual thresholds in RCS rats during photoreceptor degeneration and rescue by cell transplants. *Vision Research, 44*(1), 9–18.

Sauve, Y., Pinilla, I., & Lund, R. D. (2006). Partial preservation of rod and cone ERG function following subretinal injection of ARPE-19 cells in RCS rats. *Vision Research, 46*(8–9), 1459–1472.

Schuett, S., Bonhoeffer, T., & Hubener, M. (2002). Mapping retinotopic structure in mouse visual cortex with optical imaging. *Journal of Neuroscience, 22*(15), 6549–6559.

Sheth, S. A., Nemoto, M., Guiou, M. W., Walker, M. A., & Toga, A. W. (2005). Spatiotemporal evolution of functional hemodynamic changes and their relationship to neuronal activity. *Journal of Cerebral Blood Flow and Metabolism, 25*(7), 830–841.

Sillito, A. M. (1979). Inhibitory mechanisms influencing complex cell orientation selectivity and their modification at high resting discharge levels. *Journal of Physiology, 289*, 33–53.

Silveira, L. C., Heywood, C. A., & Cowey, A. (1987). Contrast sensitivity and visual acuity of the pigmented rat determined electrophysiologically. *Vision Research, 27*(10), 1719–1731.

Spear, P. D. (1993). Neural bases of visual deficits during aging. *Vision Research, 33*(18), 2589–2609.

Stafford, C. A. (1984). Critical period plasticity for visual function: Definition in monocularly deprived rats using visually evoked potentials. *Ophthalmic and Physiological Optics, 4*(1), 95–100.

Tomita, H., Sugano, E., Yawo, H., Ishizuka, T., Isago, H., Narikawa, S., et al. (2007). Restoration of visual response in aged dystrophic RCS rats using AAV-mediated channelopsin-2 gene transfer. *Investigative Ophthalmology and Visual Science, 48*(8), 3821–3826.

Van der Gucht, E., Hof, P. R., Van Brussel, L., Burnat, K., & Arckens, L. (2007). Neurofilament protein and neuronal activity markers define regional architectonic parcellation in the mouse visual cortex. *Cerebral Cortex, 17*(12), 2805–2819.

Vugler, A., Lawrence, J., Walsh, J., Carr, A., Gias, C., Semo, M., et al. (2007). Embryonic stem cells and retinal repair. *Mechanisms of Development, 124*(11–12), 807–829.

Wandell, B. A., & Smirnakis, S. M. (2009). Plasticity and stability of visual field maps in adult primary visual cortex. *Nature Reviews Neuroscience, 10*(12), 873–884.

Worgotter, F., & Koch, C. (1991). A detailed model of the primary visual pathway in the cat: Comparison of afferent excitatory and intracortical inhibitory connection schemes for orientation selectivity. *Journal of Neuroscience, 11*(7), 1959–1979.

Yamashita, A., Valkova, K., Gonchar, Y., & Burkhalter, A. (2003). Rearrangement of synaptic connections with inhibitory neurons in developing mouse visual cortex. *Journal of Comparative Neurology, 464*(4), 426–437.

Zhan, C. A., Ledgeway, T., & Baker, C. L. Jr., (2005). Contrast response in visual cortex: Quantitative assessment with intrinsic optical signal imaging and neural firing. *Neuroimage, 26*(2), 330–346.